Structures and Hydrogen Bonding Analysis of *N*,*N*-Dimethylformamide and *N*,*N*-Dimethylformamide−Water Mixtures by Molecular Dynamics Simulations

Yi Lei, Haoran Li,* Haihua Pan, and Shijun Han

Department of Chemistry, Zhejiang University, Hangzhou 310027, People's Republic of China

Received: July 30, 2002; In Final Form: September 23, 2002

Pure *N*,*N*-dimethylformamide (DMF) and DMF−water mixtures are studied by molecular dynamics (MD) simulations. An OPLS all-atom force field is used for the simulation of DMF, revealing the local order and formation of the weak hydrogen bond of C−H···O, and TIP5P is adopted for the simulation of water and is compared with the latest X-ray and neutron diffraction experiment. Solution properties of DMF−water mixtures are investigated using radial distribution functions (RDFs) and hydrogen bonding properties. A significant composition dependence, which is attributed to the prevailing influence of the strongly polarizable amido of DMF and the clustering feature of water, is observed in the simulation. In addition, NMR experiments of DMF−water mixtures are used for the discussion of the hydrogen bonding effect. The results of the simulation are adopted to explain the NMR experiments by hydrogen bonding analysis. As a result, the magnetic anisotropy of the amido group is considered to play an important role in the chemical shift.

1. Introduction

Amides are very interesting compounds and often serve as a model of the peptide bond. Hydration effects on the structure of such biological model molecules are important in understanding the role of water in the behavior of these molecules in biological media. The interaction plays a crucial role in the solvation of the peptides in aqueous solutions. It is increasingly recognized that the C−H···O hydrogen bond plays a significant role in determining the molecular conformation and crystal packing,[1] in the stabilization of complexes,[2] and in the activity of biological macromolecules.[3] The weak hydrogen bond, which exists widely in protein structures, may be the key to protein folding. To investigate the nature of these interactions, we performed molecular dynamics (MD) simulations in a model molecule system, *N*,*N*-dimethylformamide(DMF)−water mixtures. However, we choose this amide because it is unable to engage in N−H···O═C hydrogen bonding with dialkyl substitution at the nitrogen.

DMF liquid has been extensively studied by spectral and theoretical studies.[4−10] Furthermore, Cordeiro and Freitas have performed a Monte Carlo (MC) simulation to investigate the DMF−water interaction and the solvent effect on the stabilization of the DMF molecule in aqueous solutions.[11] But few of them concern hydrogen bonding networks of DMF−water mixtures, especially the C−H···O interaction. The present work employs MD simulation to provide information on the molecular level for the local structures in DMF and DMF−water mixtures, the hydration of the DMF solute, the association between DMF and water molecules, and the hydrogen bonding network properties.

2. Computational Method

2.1. Molecular Models. Simple rigid potential models were used for both DMF and water. The nonbonded interactions are represented by a sum of the Coulomb and Lennard-Jones terms with eq 1

$$E_{ab} = \sum_{i}^{\text{on a}} \sum_{j}^{\text{on b}} [q_i q_j e^2/r_{ij} + 4\epsilon_{ij}(\sigma_{ij}^{12}/r_{ij}^{12} - \sigma_{ij}^{6}/r_{ij}^{6})]\, f_{ij} \quad (1)$$

where E_{ab} is the interaction energy between molecules a and b. Standard combining rules are used via eq 2.

$$\sigma_{ij} = (\sigma_{ii}\sigma_{jj})^{1/2} \qquad \epsilon_{ij} = (\epsilon_{ii}\epsilon_{jj})^{1/2} \quad (2)$$

The same expression is used for intramolecular nonbonded interactions between all pairs of atoms ($i < j$) separated by three or more bonds. Furthermore, $f_{ij} = 1.0$ except for intramolecular 1,4 interactions for which $f_{ij} = 0.5$.

For water molecules, the TIP5P model is adopted. TIP5P is a new five-site, nonpolarizable water model that was fitted by Mahoney and Jorgensen on the pure liquid water properties by MC simulation and reproduces the density of liquid water accurately over a large temperature range.[12] OPLS-AA (optimized potentials for liquid simulations-all atom) was recently developed for the all-atom force field. For the DMF molecule, a modified OPLS-AA model is adopted because the original OPLS-AA model was fitted by inaccurate pure liquid properties.[9,13] *N*-methyl group parameters are somewhat changed to agree well with experimental values of the density and heat of vaporization so that OPLS-AA work will be hardly affected. Table 1 lists the potential parameters for the pure components.

Mixtures of liquids can likewise be simulated by using the interaction potentials of the pure liquids. Generally, a good description of the behavior of the pure components is not sufficient for an accurate prediction of the properties of a nonideal associated binary system such as DMF−water mixtures when simple combination rules are used for the cross interactions. Notwithstanding, the simulations of mixtures have been reasonably successful in predicting many mixed properties. The results should be viewed as providing a qualitative description

* Corresponding author. E-mail: lihr@zju.edu.cn; leiy@zju.edu.cn. Tel: +86-571-8795-2424. Fax: +86-571-8795-1895.

10.1021/jp026638+ CCC: $25.00
Published on Web 02/11/2003

TABLE 1: Potential Parameters for TIP5P and DMF

	σ (Å)		ϵ (kJ/mol)		q (in units of e)
TIP5P					
O_W	3.1200		0.6694		0.0000
H_W	0.0000		0.0000		0.2410
Lp	0.0000		0.0000		−0.2410
DMF	original	modified	original	modified	
O_F	2.960		0.210		−0.500
C (C═O)	3.750		0.105		0.500
H_F (C═O)	2.420		0.015		0.000
N	3.250		0.170		−0.140
C_M (N−CH_3)	3.500	3.300	0.066	0.087	−0.240
H_M (N−CH_3)	2.500		0.030		0.060

of DMF−water mixtures. Moreover, it remains an important task to compare the experimental and predicted properties of the mixtures.

2.2. Simulation Details. MD calculations were performed by using a modified TINKER 3.9 molecular modeling package.[14] The calculations were performed in the *NPT* ensemble at $T = 298$ K and $P = 1$ atm with a total of 216 molecules. Calculations on pure DMF and DMF−water mixtures at different concentrations were carried out. One reference simulation of TIP5P water was also carried out for verification and comparison. The bigger binary system with a molar fraction of DMF $x = 0.5$, consisting of 256 molecules of DMF and 256 molecules of water, was also calculated to examine possible system-size effects.

The equations of motion were integrated with the modified Beeman method.[15] The temperature and pressure were maintained with the Berendsen algorithm.[16] Periodical boundary conditions were applied together with a spherical cutoff. The Shake algorithm was used to constrain the bond lengths, whereas all of the other degrees of freedom remained flexible.[17] Long-range interactions were handled by the smoothing function,[9,12] which was similar to the approach used in the parametrization of DMF and TIP5P models. The energies of the initial configurations were minimized by using the MINIMIZE program in the TINKER 3.9 package. The time step was 1 fs, and configurations were saved every 0.1 ps for analysis. Then the systems were sufficiently equilibrated to ensure that there were no systematic drifts in the potential energies with time. The equilibrations were followed by monitoring the radial distribution functions (RDFs) as well as the fraction of molecules of each species that had a given number of hydrogen bonds. The statistics were collected during the last 100 ps.

3. Results and Discussion

3.1. Results of Pure DMF and Water. Thermodynamic Properties. The liquid density and heat of vaporization are important measures of the size of the molecules and the strength of their interaction.[18] Density is easy to calculate in a periodic boundary system and simultaneous provides a good test of the intermolecular forces, the cutoff criterion, and the *NPT* method used. The density is calculated from the average volume with eq 3

$$\rho = M/(0.6022 \times \langle V \rangle/N \qquad (3)$$

where ρ is the density in g cm^{-3}, M is the molecular weight, N is the number of molecules in the periodic box, V is the calculated volume in Å^3, and 0.6022 is the unit conversion factor. The heat of vaporization allows us to check directly the intermolecular energy of system, which is responsible for its state of aggregation. The heat of vaporization is well approximated from the calculated energy via eq 4,[19] where R is the gas constant and T is the absolute temperature.

TABLE 2: Calculated and Experimental Thermodynamic Properties of Pure Liquids[a]

	ΔH_{vap} (kcal/mol)		ρ (g cm^{-3})	
liquid	calcd (original)	exptl (original)	calcd (original)	exptl (original)
DMF	11.21 (10.49)[b]	11.10[c] (10.40)[d]	0.943 (0.879)[b]	0.944[c] (0.873)[d]
TIP5P	10.73	10.51[c]	0.995	0.997[c]

[a] Results at 298 K and 1 atm. [b] Results are taken from ref 9a. [c] Experimental data are taken from ref 13a. [d] Experimental data are taken from ref 13b and c.

$$\Delta H_{vap} \approx -\langle E(\mathrm{l}) \rangle/N + RT \qquad (4)$$

In Table 2, a summary of the calculated properties along with the experimental values is shown. The modified OPLS-AA model of pure DMF represents the experimental liquid density and the heat of vaporization very well. The agreement between the calculated and experimental values is also very good for the TIP5P model. The results are a little different from the original findings obtained from the MC simulation. For instance, for a system of 512 TIP5P water molecules, the density and the heat of vaporization were found to be 0.999 g cm $^{-3}$ and 10.46 kcal mol $^{-1}$, respectively.[12]

Liquid Structure. The structure of the liquid can be characterized well by RDF, $g(r)$[x−y], which gives the probability of finding an atom of type y at a distance r from an atom of type x. The atom types have been defined in Table 1. For simplicity, only those $g(r)$'s that concern the hydrogen bond in pure DMF are displayed in Figure 1. On the basis of calculated RDFs with the OPLS potential, Jorgenson and Swenson suggested that liquid DMF contains significant structure and local order because of dipole−dipole interaction.[9] Our results reinforce the above local order in view of $g(r)$[O_F−C_F] and $g(r)$[O_F−C_M], which show well-structured first peaks near 3.5 and 3.6 Å, respectively. Since the OPLS-AA model recognizes H_F and H_M as different sites instead of a single C−H group site of OPLS, $g(r)$[O_F−H_F] and $g(r)$[O_F−H_M] can be obtained and show further local order. $g(r)$[O_F−H_F] presents two significant peaks near 2.7 and 6.4 Å. $g(r)$[O_F−H_M] presents three distinct peaks near 2.9, 4.3, and 6.3 Å. The large first peak and the short bond distance in the RDFs indicate weak hydrogen bonding interactions of formyl oxygen bonded with formyl hydrogen or methyl hydrogen. Recently, the crystal structure of pure DMF has been described and shows similar local order.[5] A ring of four DMF molecules connected by weak C−H···O hydrogen bonds involving two formyl hydrogens and two methyl hydrogens was observed. The local order is quite consistent with the results of the simulation. The broad

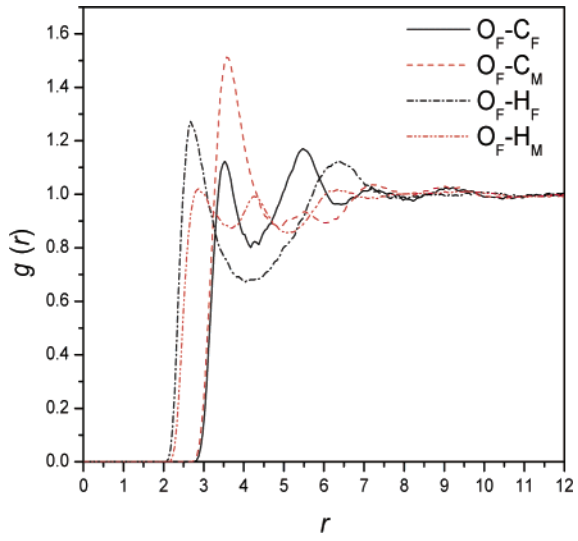

Figure 1. $g(r)$'s for pure DMF calculated with the new parameter set at 298 K and 1 atm. Distances are in angstroms. The atom types refer to those in Table 1.

first peaks of the RDFs also imply that the intermolecular interactions are likely to include hydrogen bonds as well as dispersions.

The $g(r)$'s for TIP5P are displayed in Figure 2. Our calculated $g(r)$'s are in good agreement with the previously reported results in the literature.[12] Figure 2 also shows a comparison of $g(r)[O_W-O_W]$, $g(r)[O_W-H_W]$, and $g(r)[H_W-H_W]$ of TIP5P with the latest X-ray and neutron diffraction experimental data.[20,21] $g(r)[O_W-O_W]$ values from two different experiments are in good agreement, indicating that experimental $g(r)[O_W-O_W]$ values are reliable. TIP5P gives excellent agreement with the two experimental data points, especially since the tetrahedral structure, which is measured by the second and third peaks, fits the experiments well. For $g(r)[O_W-H_W]$, TIP5P agreement more closely with experiment over the whole range but presents a higher first peak than the experiment does. For $g(r)[H_W-H_W]$, TIP5P overestimates the first peak position a little compared with experiment. TIP5P shows two peaks near 3.6 and 4.8 Å, but only one peak near 3.8 Å is observed in experiment. On the basis of the comparisons, especially $g(r)[O_W-O_W]$ values, we could conclude that TIP5P gives good descriptions of the water structure.

Hydrogen Bonding Analysis. A visual inspection of the crystal structures reveals the existence of DMF aggregates exhibiting a C−H···O hydrogen bonding type.[5] Different investigators have defined slightly different criteria for identifying the weak hydrogen bond. We adopt the somewhat modified geometrical criteria for C−H···O hydrogen bonds by comparing with Desiraju's definition, X-ray experimental data, and quantum mechanical calculation results,[1(b),5,10] specifically, $R(O\cdots H) < 2.8$, $3.0 < R(O\cdots C) < 4.0$, and the angle $C-H\cdots O > 110°$. Then, for each molecule, the probability can be calculated to have a certain number of hydrogen bonds. A summary of the statistics is given in Table 3, indicating that methyl hydrogen is a better donor than formyl hydrogen. Most formyl oxygens have one or two hydrogen bonds in their complexes, whereas few of them have more than three hydrogen bonds. The number of hydrogen bonding to two methyl hydrogens is much more than the number of hydrogen bonding to two formyl hydrogens. This implies that the interaction of the bifurcated pattern between formyl oxygen and methyl hydrogen may be more popular in DMF liquid. Because the weak hydrogen bonding force draws them together, DMF molecules tend to be fairly ordered. Vargas et al. performed a high-level ab initio calculation and located four stable DMF dimer structures in the gas phase.[10] We compare the simulation result of pure DMF liquid with Vargas' result. The four stable DMF dimers can be found, but their concentrations are small. In the majority of cases, the dimers exist in the form of linear species, not cyclic ones. Keep in mind that we are comparing the results for liquids with the ab initio calculation results for the gas phase.

Different definitions have been used to estimate the number of hydrogen bonds of water on the basis of various energetic and structure criteria.[22] Here we have adopted a geometric criterion that is the same as that used by Luzar and Chandler.[23] Two molecules are considered to be hydrogen bonded if their separations are such that $r(O\cdots H) \le 2.45$ Å, $r\,(O\cdots O) \le 3.60$ Å, and the angle $H-O\cdots O \le 30°$. With our choice of geometric criterion, 3.26 hydrogen bonds per water molecule are found in TIP5P water. Luzar and Chandler found 3.33 hydrogen bonds per water molecule using the SPC model.[23] Kalinichev performed an MC simulation to find 3.19 hydrogen bonds per water molecule using the TIP4P model.[24] Recent proton NMR chemical shift measurements from 10−40 MPa gave a scaling factor of 3.2 for the degree of hydrogen bonding.[25] Since the first peak height of $g(r)[O_W-O_W]$ is somewhat overestimated relative to the experimental data, the number of hydrogen bonds per water molecule in the TIP5P model is likely to be somewhat overestimated.

3.2. Result of DMF−Water Mixtures. Thermodynamic Properties. The DMF−water binary system exhibits strong nonideal behavior, which is reflected in its large negative excess enthalpy and volume of mixing.[26] Results for the density obtained in the simulation are compared with experimental data in Figure 3. The densities of the mixtures are reproduced fairly well qualitatively. However, the calculated values are still considerably smaller than the experimental data for high concentrations of DMF. It seems that the TIP5P model is more suitable for pure water and water-rich regions.

Liquid Structure. $g(r)[O_W-H_W]$ and $g(r)[O_F-H_W]$ are displayed in Figure 4a and b, respectively. The variations in the heights of the first peak for $g(r)[O_W-H_W]$ and $g(r)[O_W-H_W]$ in DMF−water mixtures as a function of the molar fraction of DMF are shown in Figure 5. The corresponding $g(r)[O_W-O_W]$ and $g(r)[O_F-O_W]$ show similar behavior as the concentration of DMF varies. The peak locations in RDFs are hardly affected by the concentration of DMF in Figure 4, whereas the peak amplitudes change significantly.

The increases in the peaks of RDFs between water molecules are not so much caused by an increase in the structure of water as they are by the tendency of water to remain in aggregates in the mixtures. Figure 4a shows that the first atomic coordination shells are apt to be more structured with the increase in DMF concentration in the region of $x_{DMF} < 0.750$, suggesting that the water molecules tend to form more clusters in the higher DMF concentration mixtures. However, the first atomic coordination shells are apt to be less structured, and the second coordination shells begin to vanish in $x_{DMF} > 0.750$, suggesting that the tetrahedral structures of water are rapidly destroyed. Even at high DMF concentrations, there are some water molecules that tend to reside in aggregates. Figure 4b displays two sharp peaks near 1.9 and 2.9 Å, indicating hydrogen bond formation between the formyl oxygen of DMF and the hydrogen of water. Most $g(r)[O_W-H_W]$'s exhibit the two almost equal peak amplitudes, indicating that only one hydrogen atom of the water molecule is closely related to the hydrogen bond forma-

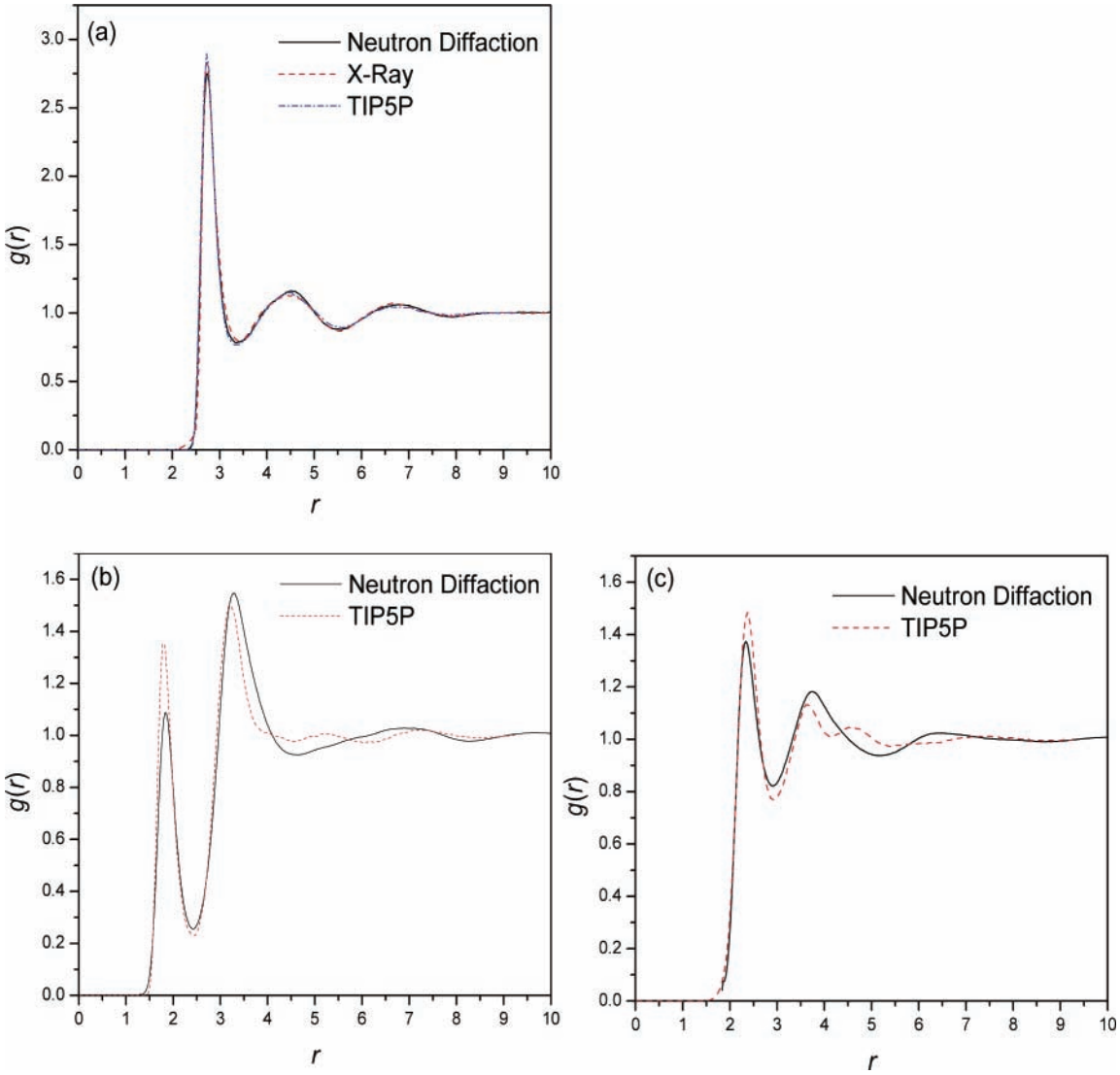

Figure 2. Calculated and experimental $g(r)$'s for pure water at 298 K and 1 atm. (a) O_W-O_W. (b) O_W-H_W. (c) H_W-H_W. Distances are in angstroms. The atom types refer to those in Table 1.

TABLE 3: Fractions (%) of O_F Atom Accepted Hydrogen Bonds to H_F and H_M Atoms in Pure DMF[a]

accepted H bonds	$O_F\cdots H_F-C_F$	$O_F\cdots H_M-C_M$
0	71.40	64.95
1	25.91	29.71
2	2.59	5.00
3	0.11	0.33
4	0.00	0.01
average	0.31	0.41

[a] The atom types refer to those in Table 1.

tion. Interestingly, DMF is found to "enhance" the structure of water in very dilute solutions of $x_{DMF} < 0.100$, whereas a further increase in DMF concentration leads to a "breakdown" of the water structure. The DMF and water molecules are apt to be more structured in $x_{DMF} > 0.750$.

In addition, some weak correlations of $O_F\cdots H_F$, $O_F\cdots H_M$, $O_W\cdots H_F$, and $O_W\cdots H_M$ are simultaneously observed, implying that there exist some weak intermolecular interactions. The "first peak height" of the weak correlation is defined to be the maximum of $g(r)$'s for $r < 2.8$ Å in order to compare with the results of hydrogen bonding analysis. Variations of the first peak height of $g(r)$'s as a function of x_{DMF} are displayed in Figure 6. These indicate a preferential conformation of the DMF−water

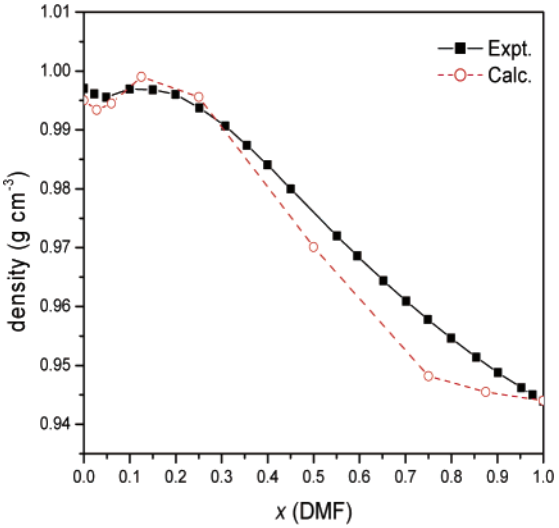

Figure 3. Calculated and experimental densities in DMF−water mixtures at 298 K and 1 atm. Experimental data are taken from ref 26.

clusters where the oxygen of the water molecule is facing a methyl group of DMF. The situation is also obtained by using

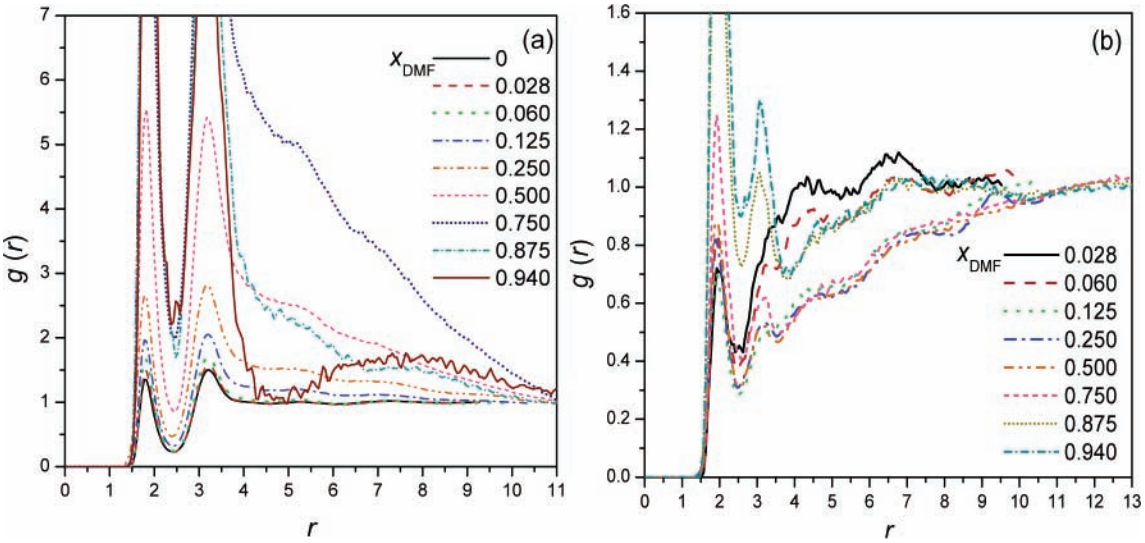

Figure 4. $g(r)$'s in DMF−water mixtures. (a) O_W-H_W. (b) O_F-H_W. Distances are in angstroms. The atom types refer to those in Table 1.

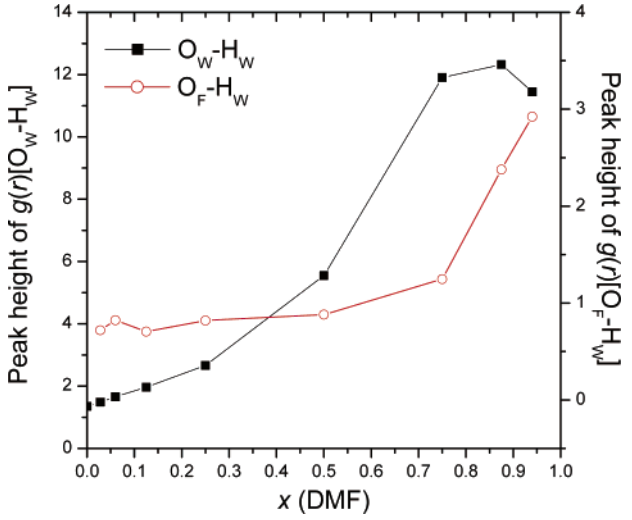

Figure 5. Variation of the first peak height of $g(r)$'s for O_W-H_W and O_F-H_W in DMF−water mixtures as a function of the molar fraction of DMF. The atom types refer to those in Table 1.

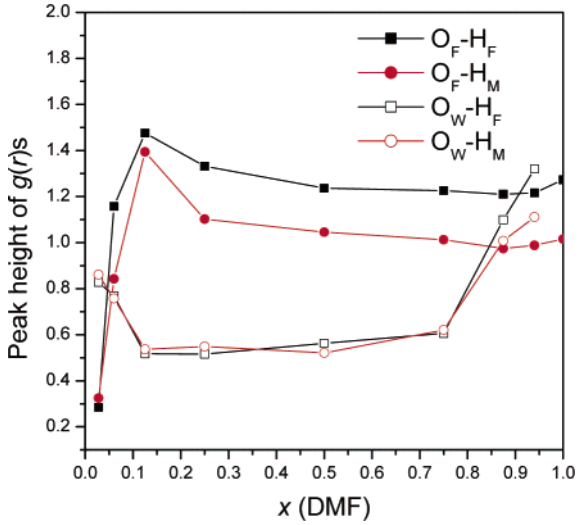

Figure 6. Variation of the first peak height of $g(r)$'s for O_F-H_F, O_F-H_M, O_W-H_F, and O_W-H_M in DMF−water mixtures as a function of x_{DMF}. The atom types refer to those in Table 1.

MD simulation in other aqueous mixtures such as acetonitrile and DMSO.[27,28]

In a general way, the higher peak amplitudes in water−water and solute−water pair correlation functions were attributed to the enhancement of the ordered structure. Although the pair correlation function is very useful for the analysis of the liquid structure sensitivity to various physical parameters such as temperature and pressure at a permanent composition, one has to be very careful when the composition of the studied mixture is changing, especially if one or more than one component is an associated liquid.[28]

Hydrogen Bonding Analysis. Since, as was shown above, RDFs do not provide explicit information on ordering in binary mixtures, we carry out a detailed analysis of hydrogen bonding network in the mixtures to gain deeper insight into the aqueous structures. One basic aspect of the hydrogen bonding network is the probability distribution, describing the number and type of hydrogen bonds that a molecule is engaged in with other molecules.

The O−H···O hydrogen bond plays a crucial role in aqueous solutions. These hydrogen bonds are determined by a similar geometrical criterion to that of pure water as defined in section 3.1, whereas the cutoff distance is taken to be the distance of the first minimum in the corresponding RDF. Water molecules can be both double donors and double acceptors of hydrogen bonds, leading ideally to tetrahedral water coordination. DMF and water compete as acceptors of hydrogen bonds, which are donated by water molecules. This leads to some rather interesting solvation effects and hydrogen bonding network in the DMF−water mixtures. A summary of the statistics is given in Figure 7.

In pure water, the state corresponding to accepting two and donating two protons is the most common. As anticipated, the average number of hydrogen bonds that the water molecules engages in decreases with increasing DMF concentration, signaling the disruption of the hydrogen bonding network. In a fluid mixture, average populations depend on both the relative concentrations of the components and the pair correlation. The latter are described by the potentials of mean force. Hence, our simultaneous observations of a diminishing number of water−water hydrogen bonds and an increasing number of water−water correlations are not inconsistent. Indeed, without the increased correlations, the water−water bonding populations would decrease faster than they do with increasing DMF concentration. For DMF molecules, most of them have only one hydrogen

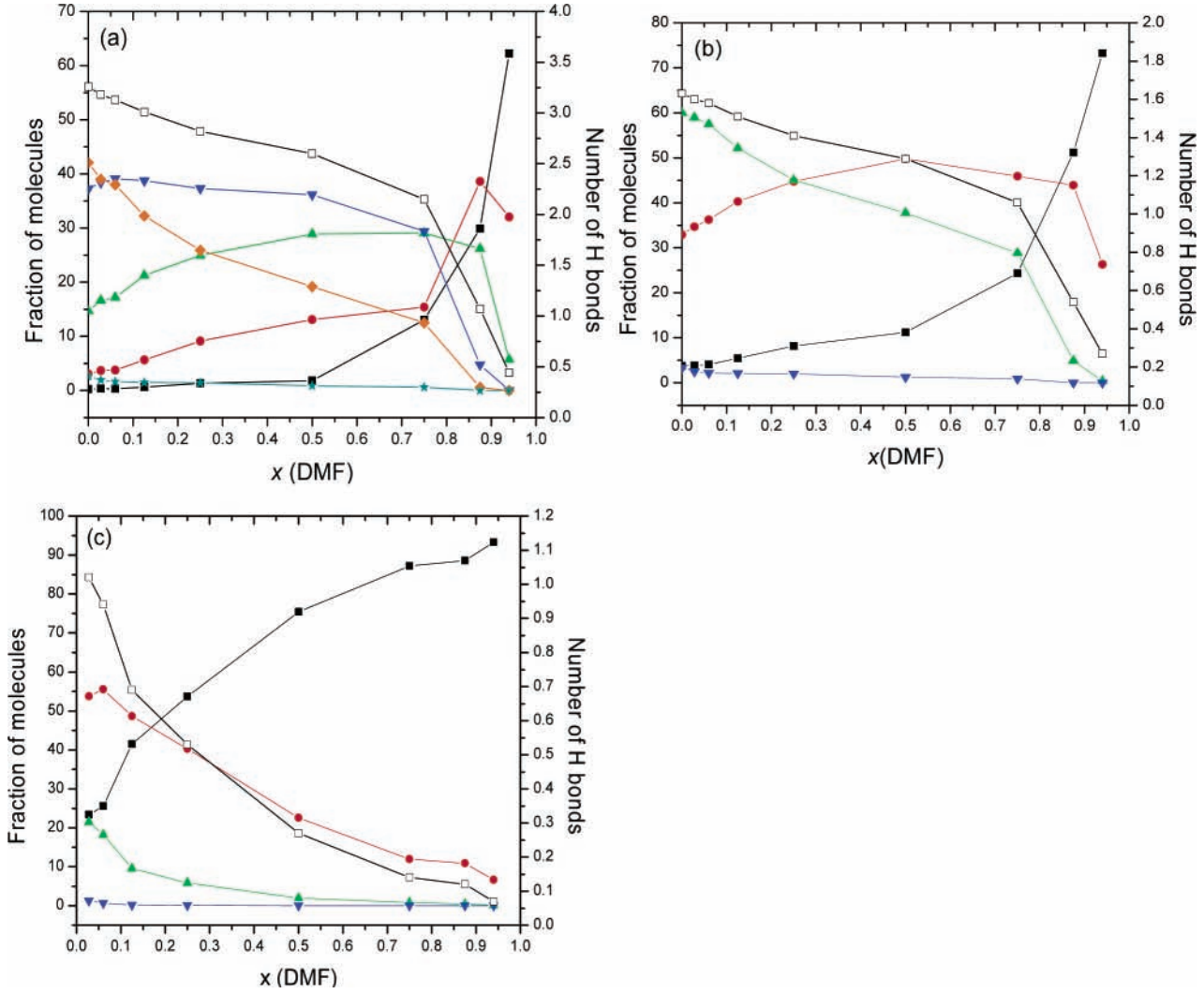

Figure 7. (a) Fraction (%) of water molecule donating and accepting zero (■), one (●), two (▲), three (▼), four (◆), and five (★) hydrogen bonds to other water molecules and the average number of hydrogen bonds (□). (b) Fraction (%) of O_W atoms accepting hydrogen bonds to H_W atoms. The symbols are same as in part a. (c) Fraction (%) of O_F atoms accepting hydrogen bonds to the H_W atom. The symbols are the same as those in part a. The atom types refer to those in Table 1.

bond to one water molecule over the entire composition range, but a small number have two hydrogen bonds to two water molecules in diluted aqueous solution. The ratios between the number hydrogen bonding to one and the number hydrogen bonding to two water molecules increase with the concentration of DMF. Therefore, the dimer DMF·H_2O seems to be more stable than the trimer DMF·$(H_2O)_2$.

According to the simulation, water molecules are hydrogen bonding to water molecules, but near the solvated DMF molecules, they can simultaneously bond with DMF or readily switch their bonds from water to DMF to form $(DMF)_m$·$(H_2O)_n$ aggregates. Some average numbers of hydrogen bonds are relatively large in $x_{DMF} < 0.10$, and the water structure breaks more quickly in $x_{DMF} > 0.75$. In DMF-rich regions, water molecules are apt to form one or two hydrogen bonds with DMF molecules and form fewer hydrogen bonds with water molecules. Because DMF molecules that hydrogen bond to water molecules appear more frequently, water clusters are easily destroyed. However, there persists some noticeable degree of hydrogen bonding, represented by small clusters such as dimers and trimers, even in systems with high concentrations of DMF.

Since the intermolecular energy of the system is described by a continuous interaction potential in the simulation, we cannot distinguish with precision whether two molecules are hydrogen bonding or not, so the adoption of a criterion to the C−H···O hydrogen bonds in DMF−water mixtures may be somewhat arbitrary. The same geometrical criteria in section 3.1 are used for DMF−water mixtures to compare with pure DMF. Notice that different criteria result in numerically different results for the extent of hydrogen bonding from the same simulation. A summary of the statistics is displayed in Figure 8. Little attention was paid to the C−H···O hydrogen bond in aqueous solution. Here, it is found that the interaction of the weak hydrogen bonds cannot be neglected. Formyl oxygen is a better acceptor than hydroxyl oxygen, and methyl hydrogen is a better acceptor than formyl hydrogen. Figure 8a and b shows that the average number of hydrogen bonds accepted by formyl oxygen increases abruptly with increasing x_{DMF} in $x_{DMF} < 0.10$. Figure 8c and d shows that the average number of hydrogen bonds accepted by hydroxyl oxygen increases abruptly with increasing x_{DMF} in $x_{DMF} > 0.75$. This indicates that the two hydrophobic C−H groups play different roles in DMF aqueous solution.

Snapshots of the configurations show that water molecules are not evenly distributed over the whole region but are apt to form some clusters. DMF−water mixtures exhibit microheterogeneity on a molecular length scale, as water-rich and DMF-rich clusters interpenetrate over an extensive range of composition.

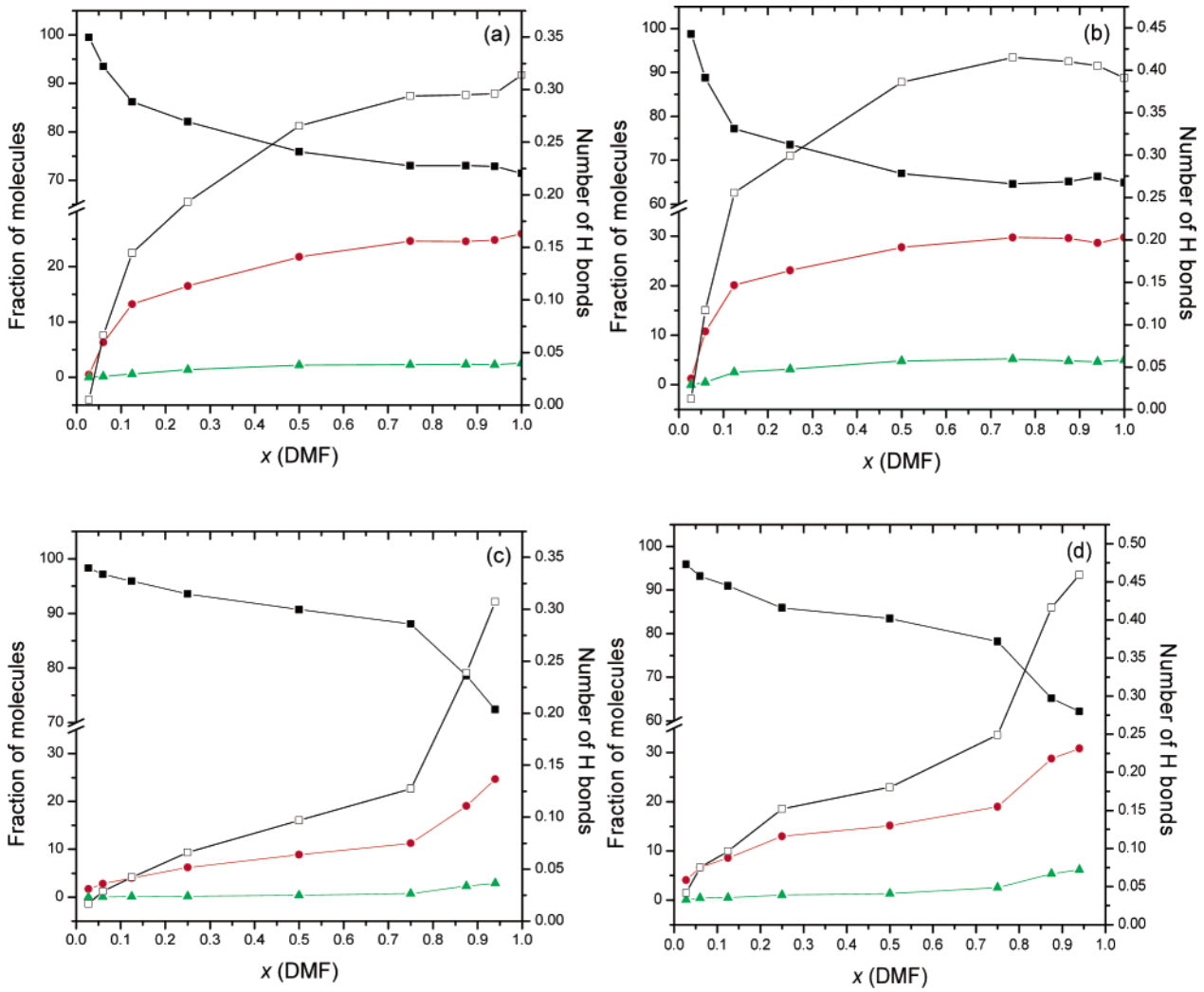

Figure 8. (a) Fraction (%) of O_F atoms accepting zero (■), one (●), and two (▲) hydrogen bonds to H_F atoms and the average number of hydrogen bonds (□). (b) Fraction (%) of O_F atoms accepting hydrogen bonds to other H_M atoms and the average number of hydrogen bonds. The symbols are the same as those in part a. (c) Fraction (%) of O_W atoms accepting hydrogen bonds to H_F atoms and the average number of hydrogen bonds. The symbols are the same as those in part a. (d) Fraction (%) of O_W atoms accepting hydrogen bonds to H_M atoms and the average number of hydrogen bonds. The symbols are the same as in part a. The atom types refer to those in Table 1.

The large system of 512 molecules has similar cluster properties to the small system of 108 DMF and 108 water molecules. Snapshots of the configurations of water molecules in the large system reveal that the large cluster is not compact like the small system, whereas the fairly dense clusters are interconnected by some sparse water molecules. Of course, the number of molecules in the clusters is different, which implies that size effects are worth considering. Computing efficiency and size effects ought to be a compromise.

Comparison with the NMR Experiment. Spectral measurements such as IR, Raman, and NMR are highly powerful techniques that may be used to investigate intermolecular interactions in solution. However, there is still very little spectral data over the whole composition range for binary mixtures, especially in aqueous mixtures. NMR and IR spectra of aqueous binary mixtures of acetone, alcohol, and DMSO have been measured.[29−31] We measured ^{1}H NMR spectra of DMF−water mixtures over the whole composition range at different temperatures.[32] ^{1}H NMR spectra were measured using a Bruker DMX500 spectrometer operating at 500 MHz at 298.0 ± 0.1 K. Chemical shifts were determined by the external double-reference method[30,33,34] using a homemade external reference tube and a capillary of 2-mm diameter with a blown-out sphere of 4-mm diameter at the bottom, which was filled with the chemical shift reference of sodium 2,2-dimethyl-2-silapentane-5-sulfonate (DSS) and set at the center of the sample tube of 5-mm diameter.

However, NMR is a quantity that is averaged over the protons of all of the molecules in the solution. The hydration of a solute in aqueous solution is not fully understood on the microscopic level. It is well known that the effect on the chemical shifts of hydrogen bonds is much larger than all of the other intermolecular interaction effects. Since the chemical shift is a measure of the electron density about the probe nuclei, it gives the information state for the atom. The chemical shift measures the changes in the electronic shell, driven by the proximity of hydrogen bonding donors and acceptors. In this regard, the chemical shift is similar to the intermolecular potential energy of MD simulations. In the planar ground-state configuration of DMF, the two NCH_3 groups are in nonequivalent magnetic environments (Figure 9). Since the energy barrier to rotation about the central C−N bond is relatively high owing to electron delocalization, two discrete NCH_3 resonances are often observed in NMR spectra.[6] In general, NCH_3(c) is at higher field than NCH_3(t). It is well recognized that the nonexchanging chemical shift, $\Delta\delta(NCH_3)$, between the two NCH_3 groups is significantly temperature-, solvent-, and concentration-dependent. The effect of concentration on $\Delta\delta(NCH_3)$ is important since studies of the

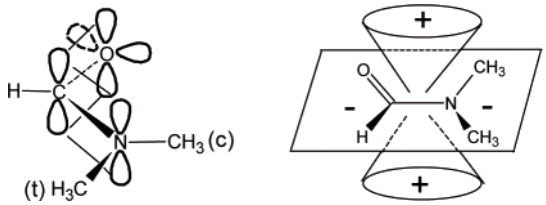

Figure 9. Nonequivalent magnetic property and magnetic anisotropy of DMF.

magnetic anisotropy of the amido (Figure 9) have been based on these relative chemical shifts. Figure 10 shows the results of the proton NMR chemical shifts compared with the average numbers of hydrogen bonds in the simulation.

The chemical shift of water protons, $\delta(H_W)$, is a measure of the electron density about the water protons, and it reflects the polarization of water molecules dissolving solutes. Since the models are more applicable in water-rich regions, we will mainly discuss those regions. Figure 10a indicates that $\delta(H_W)$ is somewhat larger than the value for pure water in $x_{DMF} < 0.10$, reaches a maximum at $x_{DMF} \approx 0.06$, and decreases rapidly with x_{DMF} in $x_{DMF} > 0.10$. The variation of the chemical shift with x_{DMF} is analogous to that of the $O_W-H\cdots O_W\&O_F$ hydrogen bond, which denotes the hydrogen bond that the H_W atom donates to the hydrogen bond to the O_W atom and the O_F atom, suggesting that the presence of the highly polarized water molecules is responsible for the O−H···O hydrogen bond between water and DMF. The larger the $\delta(H_W)$ value, the stronger the polarization and the hydrogen bonding interactions of the water molecules. Analyses of densities and partial molar excess volumes of the mixtures also lead to the similar conclusion that DMF behaves as a strong structure maker.[26] In Figure 10b, the chemical shift of formyl hydrogens, $\delta(H_F)$, increases with x_{DMF} over the whole composition range. $\delta(H_F)$ increases with increasing temperature in $x_{DMF} < 0.10$, whereas it decreases with increasing temperature in $x_{DMF} > 0.10$,[32] implying the type of intermolecular interactions of C−H group transitions from dispersion to hydrogen bonding. In Figure 10c, the nonexchanging chemical shift between the two methyl hydrogens, $\Delta\delta(H_M)$, increases rapidly with x_{DMF} in $x_{DMF} < 0.30$, whereas it increases with increasing temperature, implying that the hydrogen bonding interaction dominates the intermolecular interaction.[32] The cooperation of two kinds of hydrogen bonds, accepted by the oxygen atoms of DMF and water, results in the changes in the chemical shifts. The hydrogen bonding interactions of $O_W\cdots H_F$ and $O_W\cdots H_M$ are important in $x_{DMF} < 0.10$, whereas those of $O_F\cdots H_F$ and $O_F\cdots H_M$ become significant in $x_{DMF} > 0.100$.

The situation is analogous to that of acetone in aqueous mixtures investigated by NMR and MD simulations[29,35] but is different from that of alcohols.[30] Furthermore, the comparisons reveal that the acceptor of the amido is more effective in determining the δ values than the hydroxyl group, owing to its

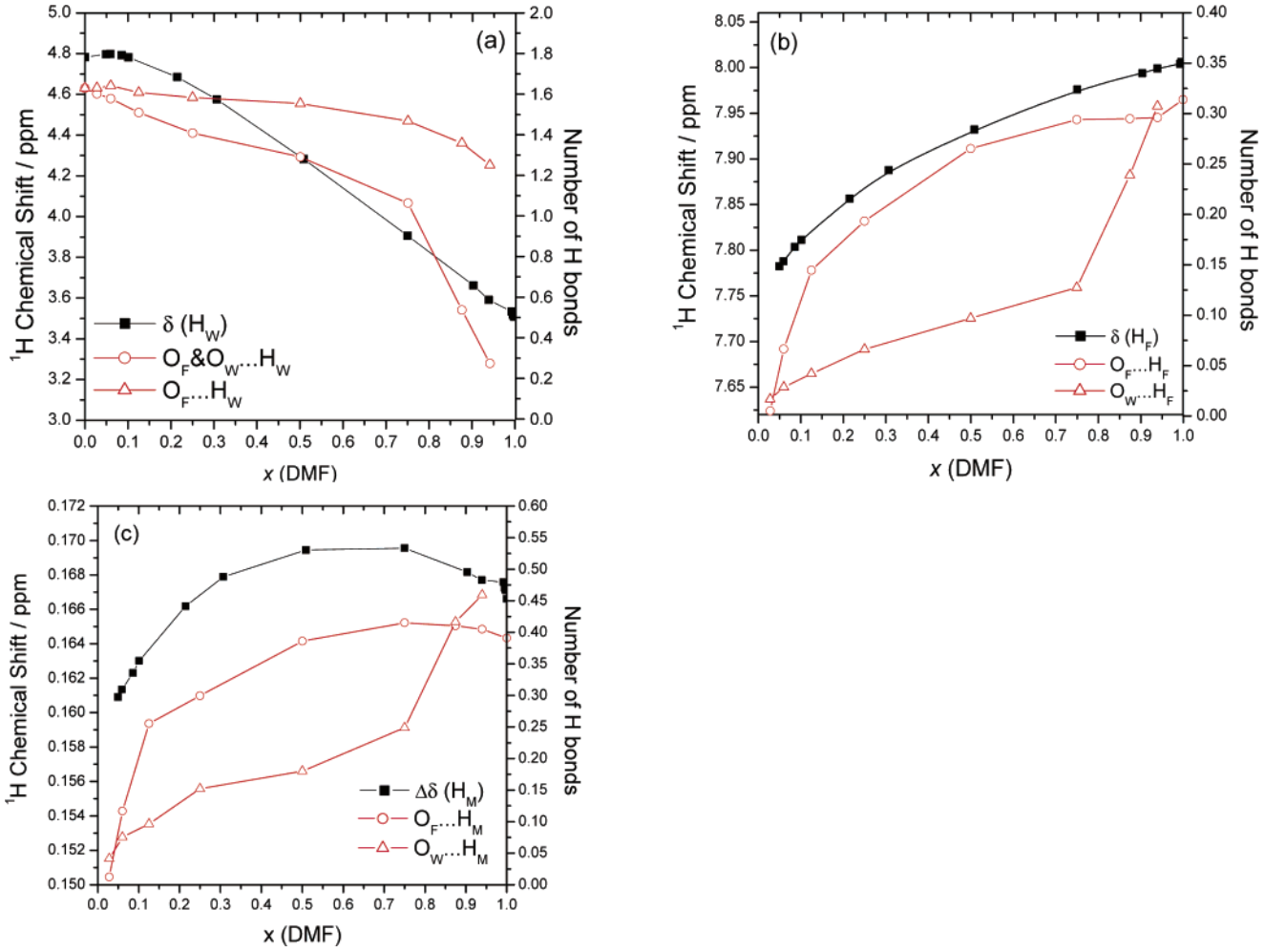

Figure 10. (a) Average numbers of $O_W-H_W\cdots O_W$ and $O_W-H_W\cdots O_W\&O_F$ hydrogen bonds donated and accepted by water molecules along with $\delta(H_W)$. (b) Average numbers of $C_F-H_F\cdots O_F$ and $C_F-H_F\cdots O_W$ hydrogen bonds along with $\delta(H_F)$. (c) Average numbers of $C_M-H_M\cdots O_F$ and $C_M-H_M\cdots O_W$ hydrogen bonds along with $\Delta\delta(H_M)$. The atom types refer to those in Table 1.

magnetic anisotropy. The ratio of DMF to water seems to be the predominant factor in the hydrophobic hydration. The polarized water is correlated not only with the interaction between water and the amido but may be also related to the hydrophobic hydration of the C−H group, especially at low concentration.

A comparison of such present results could further validate the intermolecular potentials and methods employed in the simulation. More importantly, such a scheme could be used to tie together such disparate measures of hydrogen bond as RDF and the chemical shift.

4. Conclusions

The liquid models that have been used in computer simulations can be divided into two main categories: united-atom (UA) and all-atom (AA) models. The primary advantage of the united-atom models is their computational efficiency. As computer technology develops rapidly, all-atom models give a more faithful and appropriate description of the shape of a real liquid. In addition, all-atom models allow for the distribution of partial charges on the individual hydrogen and carbon atoms, which may be important in describing the interactions of alkanes with more polar molecules. In the present study, the modified OPLS-AA model was successfully used for the simulations of pure DMF and DMF−water mixtures and demonstrated an excellent ability to reveal the detailed description of the hydrogen bonds of O−H···O as well as C−H···O, shedding light on the hydration of the C−H group.

TIP5P is also a rigid and nonpolarizable model like other SPC, TIP3P, and TIP4P models. The main difference concerns the point charges that are tetrahedrally distributed onto the two hydrogens and the two oxygen lone pairs. TIP5P was adopted for MD simulations and compared with the latest X-ray and neutron diffraction experimental data, indicating that it describes the structure and property of pure water better.

Because these simple models represent electrostatic interactions with only the Coulomb terms using fixed charges, they incorporate the polarization effects only in an average sense. Here, the nonpolarizable model yields a good qualitative description of DMF aqueous solutions but not a quantitative description. Recent developmental work on the liquid models has focused on the explicit incorporation of polarization. However, the optimal format is still under debate. The simple models will continue to receive much use in future work.

DMF−water mixtures have been investigated using MD simulation over the whole composition range and have been mainly compared with NMR experiments in the water-rich region. In NMR experiments, DMF was found to enhance the structure of water in dilute solutions, whereas a further increase in DMF concentration in the solution led to a breakdown of the water structure. Similar behavior of water RDF peaks as a function of DMF concentration was observed in the simulation. Then, both the strong O−H···O and the weak C−H···O hydrogen bonds were examined in detail. The results indicate that the DMF molecules are apt to coalesce into the water clusters to form larger ones through the strong O−H···O hydrogen bonds in water-rich region, whereas the tetrahedral structure of water is lost as DMF concentration increases and breaks more quickly in the DMF-rich region. At the same time, the hydration of the C−H group of DMF occurs through the weak C−H···O hydrogen bonds to bring on the change in the polarization of DMF solutes as well as surrounding water molecules in the water-rich region. We remark that the clustering feature of water, the strongly polarizable amido, and its magnetic anisotropy are key factors in inducing the anomalous polarization of DMF and water molecules in NMR experiments.

The present study was successful in revealing the detailed structural and hydrogen bonding properties in DMF solute molecules as well as in water solvent molecules as functions of concentration. Since a combination of MD simulation and NMR analysis was demonstrated to be useful for illustrating the cooperative effect and hydration in the aqueous solutions, we can expect it to be a powerful technique that is applicable to a variety of subjects in solution chemistry and biochemistry.

Acknowledgment. We thank Professor J. W. Ponder and Dr. P. Ren of Washington University for their help with the TINKER 3.9 molecular modeling package. We are also grateful to Dr. M. W. Mahoney of Yale University for his advice on the TIP5P water model. This work was supported by the National Natural Science Foundation of China (no. 29976035) and Zhejiang Provincial Natural Science of China (no. RC01051).

References and Notes

(1) (a) Green, R. D. *Hydrogen Bonding by C−H Groups*; Macmillan: London, 1974. (b) Desiraju, G. R. *Acc. Chem. Res.* **1996**, *29*, 441. (c) Desiraju, G. R.; Stdiner, T. *The Weak Hydrogen Bond in Structural Chemistry and Biology*; Oxford University Press: Oxford, U.K., 1999.

(2) (a) Braga, D.; Grepioni, F.; Byrne, J. J.; Wolf, A. *J. Chem. Soc., Chem. Commun.* **1995**, 125. (b) Behrens, P.; van de Goor, G.; Freyhardt, C. C. *Angew. Chem., Int. Ed. Engl.* **1995**, *34*, 2895.

(3) (a) Musah, R. A.; Jensen, G. M.; Rosenfeld, R. J.; McRee, D. E.; Goodin, D. B. *J. Am. Chem. Soc.* **1997**, *119*, 9083. (b) Rouhi, M. *Chem. Eng. News* **2002**, *78*, 15.

(4) Henson, D. B.; Swenson, C. A. *J. Phys. Chem.* **1973**, *77*, 2401.

(5) Borrman, H.; Persson, I.; Sandström, M.; Stalhandske, C. M. V. *J. Chem. Soc., Perkin Trans. 2* **2000**, 393.

(6) Neuman, R. C., Jr.; Snider, W.; Jonas, V. *J. Phys. Chem.* **1968**, *72*, 2469.

(7) Gao, J.; Pavelites, J. J.; Habibollazadeh, D. *J. Phys. Chem.* **1996**, *100*, 2689.

(8) Desfrancois, C.; Periquet, V.; Varles, S.; Schermann, J. P.; Adamowics, L. *Chem. Phys.* **1998**, *239*, 475.

(9) (a) Jorgensen, W. J.; Swenson, C. J. *J. Am. Chem. Soc.* **1985**, *107*, 569, 1469. (b) Jorgensen, W. J.; Maxwell D. S.; Tirado-Rives, J. *J. Am. Chem. Soc.* **1996**, *118*, 11225.

(10) Vargas, R.; Garza, J.; Dixon D. A.; Hay B. P. *J. Am. Chem. Soc.* **2000**, *122*, 4750.

(11) Cordeiro, J. M. M.; Freitas, L. C. G. *Z. Naturforsch., A: Phys. Sci.* **1999**, *54*, 110.

(12) Mahoney, M. W.; Jorgensen, M. L. *J. Chem. Phys.* **2000**, *112*, 8910.

(13) (a) *CRC Handbook of Chemistry and Physics*, 80th ed.; Lide, D. R., Ed.; CRC Press: Boca Raton, FL, 1999−2000. (b) *DMF Product Bulletin*; E. I. duPont, Inc.: Wilmington, DE, 1971. (c) Zegers, H. C.; Somsen, G. *J. Chem. Thermodyn.* **1984**, *16*, 225.

(14) Dudek, M. J.; Ramnarayan, K.; Ponder, J. W. *J. Comput. Chem.* **1998**, *19*, 548.

(15) Brooks, B. R. In *Algorithms for Molecular Dynamics at Constant Temperature and Pressure*; DCRT Report; National Institutes of Health: Bethesda, MD, April 1988.

(16) Berendsen, H. J. C.; Postma, J. P. M.; Van Gunsteren, W. F. *J. Chem. Phys.* **1984**, *81*, 3684.

(17) Andersen, H. C. *J. Comput. Phys.* **1983**, *52*, 24.

(18) Jorgensen, W. L. In *The Encyclopedia of Computational Chemistry*; Schleyer, P. V. R., Allinger, N. L., Clark, T., Gasteiger, J., Kollman, P. A., Schaefer, H. F., Eds.; John Wiley & Sons Ltd.: Chichester, U.K., 1998; p 1754.

(19) Jorgensen, W. L.; Madura, J. D. *Mol. Phys.* **1985**, *56*, 1381.

(20) Sorenson, J. M.; Hura, G.; Glaeser, R. M.; Head-Gordon, T. *J. Chem. Phys.* **2000**, *113*, 9149.

(21) Soper, A. K. *Chem. Phys.* **2000**, *258*, 121.

(22) Mezei, M. *Phys. Many-Body Systems* **1991**, *19*, 37.

(23) Luzar, A.; Chandler, D. *J. Chem. Phys.* **1993**, *98*, 8160.

(24) Kalinichev, A. G.; Bass, J. D. *J. Phys. Chem. A* **1997**, *101*, 9726.

(25) Hoffmann, M. M.; Conradi, M. S. *J. Am. Chem. Soc.* **1997**, *119*, 3811.

(26) Miyai, K.; Nakamura, M.; Tamura, K.; Murakami, S. *J. Solution Chem.* **1997**, *26*, 973.
(27) Kovacs, H.; Laaksonen, A. *J. Am. Chem. Soc.* **1991**, *113*, 5596.
(28) Vaisman, I. I.; Berkowitz, M. L. *J. Am. Chem. Soc.* **1992**, *114*, 7889.
(29) Mizuno, K.; Ochi, T.; Shindo, Y. *J. Chem. Phys.* **1998**, *109*, 9502.
(30) Mizuno, K.; Kimura, Y.; Morichika, H.; Nishimura, Y.; Shimada, S.; Maeda, S.; Imafuji, S.; Ochi, T. *J. Mol. Liq.* **2000**, *85*, 139.
(31) Mizuno, K.; Imafuji, S.; Ochi, T.; Ohta, T.; Maeda, S. *J. Phys. Chem. B* **2000**, *104*, 11001.
(32) Lei, Y.; Li, H.; Zhu, L.; Han, S. *Acta Chim. Sin.* **2002**, *60*, 1747.
(33) Momoki, K.; Fukazawa, Y. *Anal. Chem.* **1990**, *62*, 1665.
(34) Momoki, K.; Fukazawa, Y. *Anal. Sci.* **1994**, *10*, 53.
(35) Venables, D. S.; Schmuttenmaer, C. A. *J. Chem. Phys.* **2000**, *113*, 9502.